



Steady-state fluctuation relations for systems driven by an external random force

To cite this article: J. R. Gomez-Solano *et al* 2010 *EPL* **89** 60003

View the [article online](#) for updates and enhancements.

You may also like

- [Manipulating plasma turbulence in cross-field plasma sources using unsteady electrostatic forcing](#)
Benedict I Rose and Aaron Knoll
- [Partial entropy production in heat transport](#)
Deepak Gupta and Sanjib Sabhapandit
- [Effect of depth ratio on Faraday instability in a binary liquid system](#)
K P Choudhary, S P Das and Shaligram Tiwari

Steady-state fluctuation relations for systems driven by an external random force

J. R. GOMEZ-SOLANO^(a), L. BELLON, A. PETROSYAN and S. CILIBERTO

Université de Lyon, Laboratoire de Physique, Ecole Normale Supérieure de Lyon, CNRS - 46, Allée d'Italie, 69364 Lyon Cedex 07, France, EU

received 8 December 2009; accepted in final form 10 March 2010

published online 19 April 2010

PACS 05.40.-a – Fluctuation phenomena, random processes, noise, and Brownian motion

Abstract – We experimentally study the fluctuations of the work done by an external Gaussian random force on two different stochastic systems coupled to a thermal bath: a colloidal particle in an optical trap and an atomic-force microscopy cantilever. We determine the corresponding probability density functions for different random forcing amplitudes ranging from a small fraction to several times the amplitude of the thermal noise. In both systems for sufficiently weak forcing amplitudes the work fluctuations satisfy the usual steady-state fluctuation theorem. As the forcing amplitude drives the system far from equilibrium, deviations of the fluctuation theorem increase monotonically. The deviations can be recasted to a single master curve which only depends on the kind of stochastic external force.

Copyright © EPLA, 2010

Introduction. – Fluctuation relations are a very important theoretical result for the description of non-equilibrium microscopic systems since they quantify the statistical properties of fluctuating energy exchanges under rather general conditions [1]. In particular, the so-called fluctuation theorem (FT) [2,3] quantifies the asymmetry of the distribution of positive and negative fluctuations of a given time-integrated quantity (injected work, entropy production, etc.). For a system in contact with a thermostat at temperature T and driven by an external force in a non-equilibrium steady state, the FT states that the ratio of the probability of finding a positive fluctuation with respect to that of the corresponding negative value for the work W_τ done by the force during a time interval τ satisfies

$$\ln \frac{P(W_\tau = W)}{P(W_\tau = -W)} \rightarrow \frac{W}{k_B T}, \quad \tau \gg \tau_c, \quad (1)$$

where τ_c is the longest characteristic relaxation time of the system. Equation (1) has been tested in several experiments such as fluidized granular media [4], a colloidal particle dragged by an optical trap [5], electrical circuits [6], mechanical harmonic oscillators [7] and a colloidal particle near the stochastic resonance [8]. New fluctuation relations have been proposed as well for the entropy production [9] or by considering modifications of the statistical properties of the thermal bath [10–12]. In

all of these examples the force which drives the system out of equilibrium is inherently deterministic. However, it has been recently argued that the nature (deterministic or stochastic) of the forcing can play an important role in the distribution of the injected work leading to possible deviations from the relation (1) for large fluctuations ($W_\tau / \langle W_\tau \rangle > 1$). Indeed, it has been found in experiments and simulations such as a Brownian particle in a Gaussian white [13] and colored [14] noise bath, turbulent thermal convection [15], wave turbulence [16], a vibrating metallic plate [17], an RC electronic circuit [18] and a gravitational wave detector [19] that the probability density functions of the work done by a stochastic force are not Gaussian but asymmetric with two exponential tails leading to violations of the FT in the form of effective temperatures or non-linear relations between the left- and the right-hand side of eq. (1). It is important to remark that in the systems previously cited the steady-state FT is violated because in such a case the external random force acts itself as a kind of thermal bath. One question which naturally arises is what the work fluctuation relations will become when in addition to the external random forcing a true thermalization process is allowed. In this situation there are two sources of work fluctuations: the external force and the thermal bath. As pointed out in [12,17], one is interested in the distribution of the work fluctuations done by the external random force in the presence of a thermostat and the conditions under which the FT could be valid.

^(a)E-mail: juan.gomez_solano@ens-lyon.fr

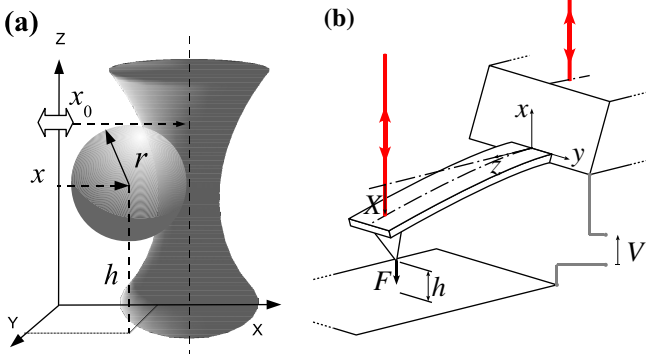


Fig. 1: (Colour on-line) a) Colloidal particle in the optical trap with modulated position. b) AFM cantilever close to a metallic surface. See text for explanation.

In the present work we address these questions in two experimental systems: a Brownian particle in an optical trap and a micro-cantilever used for atomic-force microscopy (AFM). Both are in contact with a thermal bath and driven out of equilibrium by an external random force whose amplitude is tuned from a small fraction to several times the amplitude of the intrinsic thermal fluctuations exerted by the thermostat.

Colloidal particle in an optical trap. – The first system we study consists on a spherical silica bead of radius $r = 1 \mu\text{m}$ immersed in ultrapure water which acts as a thermal bath. The experiment is performed at a room temperature of $27 \pm 0.5^\circ\text{C}$ at which the dynamic viscosity of water is $\eta = (8.52 \pm 0.10) \times 10^{-4} \text{ Pa}\cdot\text{s}$. The motion of the particle is confined by an optical trap which is created by tightly focusing a Nd:YAG laser beam ($\lambda = 1064 \text{ nm}$) by means of a high-numerical-aperture objective ($63\times$, $\text{NA} = 1.4$). The trap stiffness is fixed at a constant value of $k = 5.4 \text{ pN}/\mu\text{m}$. The particle is kept at $h \approx 10 \mu\text{m}$ above the lower cell surface to avoid hydrodynamic interactions with the walls. Figure 1(a) sketches the configuration of the bead in the optical trap. An external random force is applied to the particle by modulating the position of the trap $x_0(t)$ using an acousto-optic deflector, along a fixed direction \mathbf{x} on the plane perpendicular to the beam propagation ($+\mathbf{z}$). The modulation corresponds to a Gaussian Ornstein-Uhlenbeck noise of mean $\langle x_0(t) \rangle = 0$ and covariance $\langle x_0(s)x_0(t) \rangle = A \exp(-|t-s|/\tau_0)$. The correlation time of the modulation is set to $\tau_0 = 25 \text{ ms}$, whereas the value of its amplitude A is tuned to control the driving intensity. We determine the particle barycenter (x, y) by image analysis using a high-speed camera at a sampling rate of 1 kHz with an accuracy better than 10 nm . See ref. [20] for more details about the experimental apparatus. The attractive force exerted by the optical trap on the bead at time t along \mathbf{x} is given by $-k(x(t) - x_0(t))$. Hence, for the experimentally accessible timescales the dynamics of the coordinate x is described by the overdamped Langevin equation

$$\gamma \dot{x} = -kx + \zeta_T + f_0. \quad (2)$$

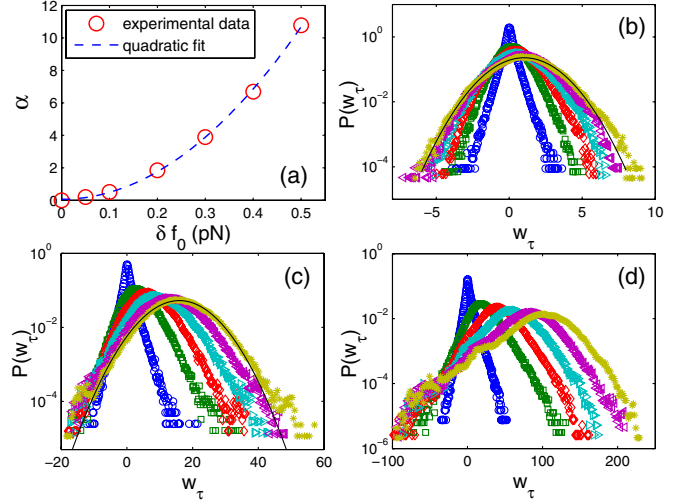


Fig. 2: (Colour on-line) (a) Dependence of the parameter α on the standard deviation of the Gaussian exponentially correlated external force f_0 acting on the colloidal particle. (b) Probability density functions of the work w_τ for $\alpha = 0.20$; (c) $\alpha = 3.89$; and (d) $\alpha = 10.77$. The symbols correspond to integration times $\tau = 5 \text{ ms}$ (\circ), 55 ms (\square), 105 ms (\diamond), 155 ms (\triangleright), 205 ms (\triangleleft) and 255 ms ($*$). The solid black lines in (b) and (c) are Gaussian fits.

In eq. (2) $\gamma = 6\pi r\eta$ is the viscous drag coefficient, ζ_T is a Gaussian white noise ($\langle \zeta_T \rangle = 0$, $\langle \zeta_T(s)\zeta_T(t) \rangle = 2k_B T \gamma \delta(t-s)$) which mimics the collisions of the thermal bath particles with the colloidal bead and $f_0(t) = kx_0(t)$ plays the role of the external stochastic force. The standard deviation δf_0 of f_0 is chosen as the main control parameter of the system. Besides the correlation time τ_0 of f_0 there is a second characteristic timescale in the dynamics of eq. (2): the viscous relaxation time in the optical trap $\tau_\gamma = \gamma/k = 3 \text{ ms} < \tau_0$. In order to quantify the relative strength of the external force with respect to the thermal fluctuations, we introduce a dimensionless parameter which measures the distance from equilibrium:

$$\alpha = \frac{\langle x^2 \rangle}{\langle x^2 \rangle_{eq}} - 1, \quad (3)$$

where $\langle x^2 \rangle$ is the variance of x in the presence of $f_0 > 0$ whereas $\langle x^2 \rangle_{eq} = k_B T/k$ is the corresponding variance at equilibrium ($f_0 = 0$). The dependence of α on δf_0 is quadratic, as shown in fig. 2(a). This quadratic dependence is a consequence of the linear response of the system to the external forcing described by the Langevin eq. (2).

The work done by the external random force on the colloidal particle (in $k_B T$ units) is

$$w_\tau = \frac{1}{k_B T} \int_t^{t+\tau} \dot{x}(t') f_0(t') dt'. \quad (4)$$

Thus, by measuring simultaneously the time evolution of the barycenter position of the particle and the driving force we are able to compute directly the work injected

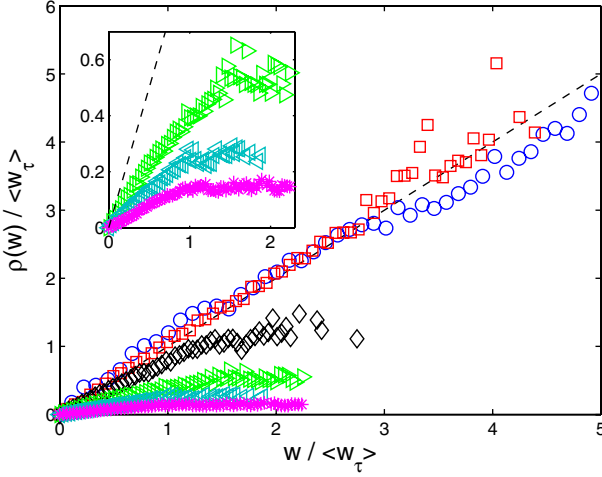


Fig. 3: (Colour on-line) Asymmetry function of the PDF of the work done by the external force on the colloidal bead computed at $\tau = 10\tau_0$ for different values of the parameter α : 0.20(\circ), 0.51(\square), 1.84(\diamond), 3.89(\triangleright), 6.69(\triangleleft), 10.77($*$). The dashed line represents the prediction of the fluctuation theorem $\rho(w) = w$. Inset: Expanded view for $\alpha \geq 3.89$.

into the system by the driving. In figs. 2(b)–(d) we show the probability density functions (PDF) of w_τ for different values of τ and α . We observe that for a fixed value of α , the PDFs have asymmetric exponential tails at short integration times and they become smoother as the value of τ increases. For $\alpha = 0.20$ they approach a Gaussian profile (fig. 2(b)) whereas asymmetric non-Gaussian tails remain for increasing values of α . Note that asymmetric non-Gaussian PDFs of the work are common in driven non-linear systems [8,21] and systems driven by a stochastic force [16–19]. As shown in figs. 2(c), (d), the asymmetry of these tails becomes very pronounced for large $\alpha > 1$ even for integration times as long as $\tau = 250\text{ ms} = 10\tau_0$, where we have taken τ_0 because it is the largest correlation time of the dynamics. The origin of this non-Gaussianity can be traced back to the strong correlation between the fluctuations of the particle motion and the stochastic external driving as α increases. As pointed out in [18], the deviations of the linear relation of eq. (1) (with respect to w_τ) can occur for extreme values of the work fluctuations located on the non-Gaussian tails.

We define the asymmetry function of the PDF P as

$$\rho(w) = \lim_{\tau_c \rightarrow \infty} \ln \frac{P(w_\tau = w)}{P(w_\tau = -w)}, \quad (5)$$

so that eq. (1) reads

$$\rho(w) = w. \quad (6)$$

From the experimental PDFs of w_τ we compute $\rho(w)$ as the logarithm in eq. (5) for integration times $\tau = 10\tau_0$. We checked that for this value the limit of eq. (5) has been attained. Figure 3 shows the profile of the asymmetry functions for different values of α . We notice that for

sufficiently small values ($\alpha = 0.20, 0.51 < 1$), the FT given by eq. (6) is verified by the experimental data. To our knowledge, this is the first time that the FT holds for a random force without introducing any prefactor in the linear relation of eq. (6). It is important to point out that any deviation from the linear relation of eq. (6) for extreme fluctuations is unlikely since we probed values as large as $w_\tau / \langle w_\tau \rangle \sim 5$. Indeed it is argued [12–14,18], that, for strongly dissipative systems driven by a random force, the deviations from FT may occur around $w_\tau / \langle w_\tau \rangle \sim 1$. Furthermore in the present case the validity of the FT for weak driving amplitudes $\alpha < 1$ is consistent with the fact that for integration times $\tau > 25\text{ ms}$, the ratio $\rho(w)/w$ has converged to its asymptotic value 1 for all measurable w . Note that this convergence to the FT prediction is quite similar to that measured in system driven out of equilibrium by deterministic forces [6–8]. For instance in the case of a harmonic oscillator driven by a sinusoidal external force the asymptotic value of $\rho(w)/w$ is reached for integration times larger than the forcing period [7].

In contrast, deviations from eq. (6) are expected to occur for $\alpha > 1$ because the fluctuations of injected energy produced by the external random force become larger than those injected by the thermal bath. Indeed fig. 3 shows that for values above $\alpha = 1.84$, eq. (6) is not verified any more but ρ becomes a non-linear function of w_τ . For small values of w_τ it is linear with a slope which decreases as the driving amplitude increases whereas there is a crossover to a slower dependence around $w_\tau / \langle w_\tau \rangle \sim 1$, a qualitatively similar behavior to those reported in [13,16–19]. We finish this section by emphasizing that we have clearly found that for an experimental system whose dynamics correspond to a first-order Langevin equation subjected to both thermal and external noises, the FT can be satisfied or not depending on the strength of the external driving. The details about how this deviations arise and the convergence to generic work fluctuation relations will be given further. We first analyze the experiment on the AFM.

AFM cantilever. – A second example of a system for which thermal fluctuations are non-negligible in the energy injection process at equilibrium is the dynamics of the free end of a rectangular micro-cantilever used in AFM measurements. The cantilever is a mechanical clamped-free beam, which can be bended by an external force F and is thermalized with the surrounding air. The experiment is sketched in fig. 1(b).

We use conductive cantilevers from Nanoworld (PPP-CONTpt). They exhibit a nominal rectangular geometry: $450\mu\text{m}$ long, $50\mu\text{m}$ wide and $2\mu\text{m}$ thick, with a 25 nm PtIr₅ conductive layer on both sides. The deflection is measured with a homemade interferometric deflection sensor [22], inspired by the original design of Schonenberger [23] with a quadrature phase detection technique [24]: the interference between the reference laser beam reflecting on the chip of the cantilever and

the sensing beam on the free end of the cantilever gives a direct measurement of the deflection X . Our detection system has a very low intrinsic noise, as low as 4 pm rms in the 100 kHz bandwidth we are probing [22,25].

From the power spectrum of the deflection fluctuations of the free end at equilibrium ($F=0$) we verify that the cantilever dynamics can be reasonably modeled as a stochastic harmonic oscillator with viscous dissipation [25,26]. Hence, in the presence of the external force the dynamics of the vertical coordinate X of the free end is described by the second-order Langevin equation

$$m\ddot{X} + \gamma\dot{X} = -kX + \zeta_T + F, \quad (7)$$

where m is the effective mass, γ the viscous drag coefficient, k the stiffness associated to the elastic force on the cantilever and ζ_T models the thermal fluctuations. m , γ and k can be calibrated at zero forcing using fluctuation dissipation theorem, relating the observed power spectrum of X to the harmonic-oscillator model: in our experiment we measure $m = 2.75 \times 10^{-11}$ kg, $\gamma = 4.35 \times 10^{-8}$ kg/s and $k = 8.05 \times 10^{-2}$ N/m. The amplitude of the equilibrium thermal fluctuations of the tip position (*i.e.* $\sqrt{\langle x^2 \rangle_{eq}} = \sqrt{k_B T/k} \simeq 2 \cdot 10^{-10}$ m) is two orders of magnitude larger than the detection noise (*i.e.* 4 pm rms). The signal-to-noise ratio is even better when the system is driven by an external force F . The characteristic timescales of the deflection dynamics are the resonance period of the harmonic oscillator $\tau_k = 2\pi\sqrt{m/k} = 116 \mu\text{s}$ and the viscous relaxation time $\tau_\gamma = m/\gamma = 632 \mu\text{s}$, which is the longest correlation time.

When a voltage V is applied between the conductive cantilever and a metallic surface brought close to the tip ($h \sim 10 \mu\text{m}$ apart), an electrostatic interaction is created. The system behaves as a capacitor with stored energy $E_c = \frac{1}{2}C(X)V^2$, with C the capacitance of the cantilever-tip/surface system. Hence, the interaction between the cantilever and the opposite charged surface gives rise to an attractive external force $F = -\partial_X E_c = -aV^2$ on the free end, with $a = \partial_X C/2$. If we apply a static voltage \bar{V} , the force F can be deduced from the stationary solution of eq. (7): $k\bar{X} = -a\bar{V}^2$, where \bar{X} is the mean measured deflection. k being already calibrated, we validate this quadratic dependence¹ of forcing in V and measure $a = 1.49 \times 10^{-11}$ N/V².

As the electrostatic force F is only attractive, its mean value cannot be chosen to be 0. We thus generated a driving voltage V designed to create a Gaussian white noise forcing f_0 around an offset \bar{F} : $F = \bar{F} + f_0$. The variance δf_0 of f_0 is the main control parameter of the system. In the absence of fluctuations ζ_T and f_0 , eq. (8) has the stationary solution $\bar{X} = \bar{F}/k$. This solution corresponds to the mean position attained by the free end in the presence of the zero mean fluctuating forces. Hence,

¹The quadratic dependence is valid only after taking care to compensate for the contact potential between the tip and the sample, which gives a small correction of the order of a few tens of mV.

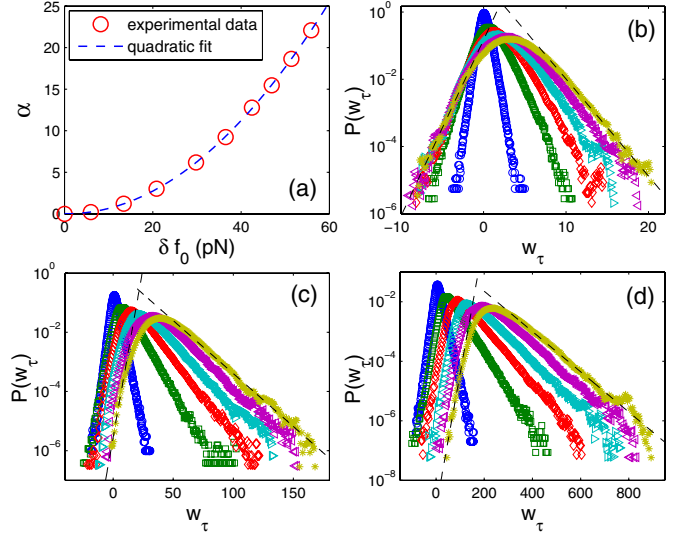


Fig. 4: (Colour on-line) (a) Dependence of the parameter α on the standard deviation of the Gaussian white external force f_0 acting on the cantilever. (b) Probability density functions of the work w_τ for $\alpha = 0.19$; (c) $\alpha = 3.03$; and (d) $\alpha = 18.66$. The symbols correspond to integration times $\tau = 97 \mu\text{s}$ (o), 1.074 ms (\square), 2.051 ms (\diamond), 3.027 ms (\triangleright), 4.004 ms (\trianglerightleft) and 4.981 ms (*). The black dashed lines in (b)–(d) represent the exponential fits of the corresponding tails.

we focus on the dynamics of the fluctuations $x = X - \bar{X}$ around \bar{X} which are described by the equation

$$m\ddot{x} + \gamma\dot{x} = -kx + \zeta_T + f_0. \quad (8)$$

Figure 4(a) shows the dependence between the parameter α defined in eq. (3) for the stochastic variable x and the control parameter δf_0 . We find that this dependence is quadratic verifying the linearity of the stochastic dynamics of the free end of the cantilever. On the other hand, the work done by the external random force during an integration time τ is computed from eq. (4). The corresponding PDFs are shown in figs. 4(b)–(d). Unlike the colloidal particle, the PDFs do not converge to a Gaussian distribution but to a profile with asymmetric exponential tails even for the smallest driving amplitude ($\alpha = 0.19$) and for integration times as long as $\tau = 8\tau_\gamma$, as shown in figs. 4(b)–(d). Surprisingly, when computing the asymmetry function for $\alpha = 0.19 < 1$ and $\tau = 4\tau_\gamma$ the steady-state FT of eq. (6) is perfectly verified, as shown in fig. 5. Work fluctuations as large as 2.5 times their mean value located on the exponential tails are probed and hence deviations from FT are unlikely for the same reasons discussed for the case of the Brownian particle.

In fig. 5 we see that for $\alpha \geq 1.21$, the deviations from eq. (6) appear as a non-linear relation with a linear part for small fluctuations whose slope decreases as α increases and a crossover for larger fluctuations, qualitatively similar to the behavior observed for the colloidal particle, as shown clearly in the inset of fig. 5. In the following we discuss

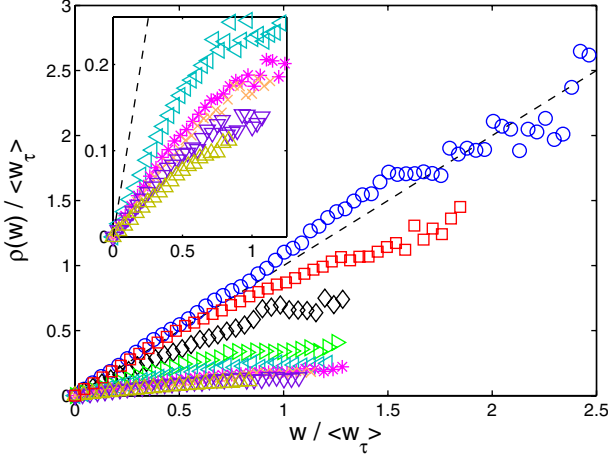


Fig. 5: (Colour on-line) Asymmetry function of the probability density function of the work done by the external force on the AFM cantilever computed at $\tau = 4\tau_\gamma$ for different values of the parameter α : 0.19 (\circ), 1.21 (\square), 3.03 (\diamond), 6.18 (\triangleright), 9.22 (\triangleleft), 12.77 ($*$), 15.46 (\times), 18.66 (∇), 22.10 (\triangle). The dashed line corresponds to the prediction of the fluctuation theorem $\rho(w) = w$. Inset: expanded view for $\alpha \geq 9.22$.

the properties of these deviations as the energy injection process becomes dominated by the external force.

Fluctuation relations far from equilibrium. – We address now the question of how the deviations from eq. (6) arise as the external stochastic force drives the system far from equilibrium. As shown previously, for $\alpha \gtrsim 1$, the forcing amplitude is strong enough to destroy the conditions for the validity of the FT for w_τ . We note that there are two well-defined limit regimes depending on the driving amplitude: one occurring at small values of α for which the steady-state FT is valid, and the limit $\alpha \gg 1$ for which the role of the thermal bath must be negligible in the energy injection process, which must be completely dominated by the external stochastic force. In order to investigate whether the transition between these two regimes is abrupt or not, we proceed by noting that for the latter the stochastic force term ζ_T in eqs. (2) and (8) will be negligible compared to f_0 . This implies that the resulting statistical time-integrated properties of the corresponding non-equilibrium steady state will be invariant under a normalization of the timescales and the temperature of the system. In particular, the resulting fluctuation relations for w_τ must lead to a master curve for the asymmetry function in the far-from-equilibrium limit $\alpha \gg 1$. The information about the transition of the fluctuation relations to this regime is given by the convergence to the master curve.

We introduce the normalized work w_τ^* as

$$w_\tau^* = \frac{\tau_c}{\tau} \frac{w_\tau}{1 + \alpha}. \quad (9)$$

The physical idea behind this normalization is that for $\alpha \gg 1$, the thermal bath alone works as a heat reservoir for

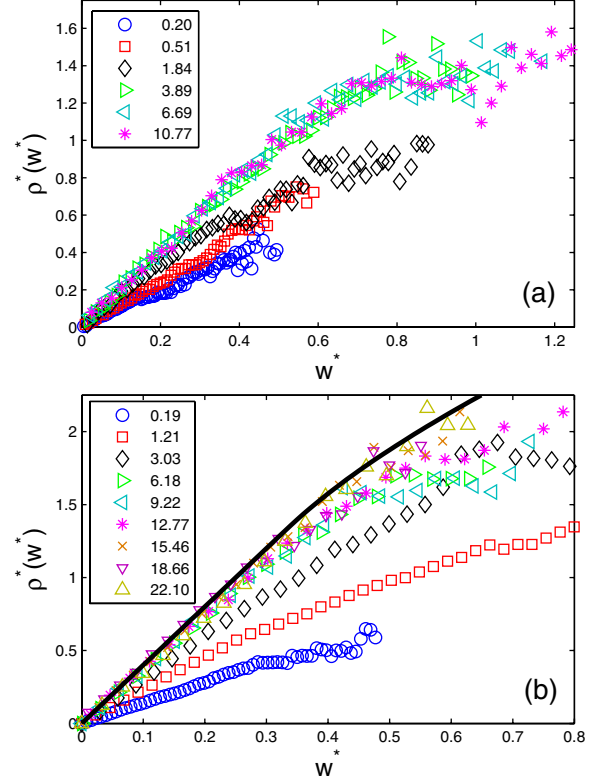


Fig. 6: (Colour on-line) (a) Asymmetry function of the PDF of the normalized work done by the Gaussian Ornstein-Uhlenbeck force on the colloidal particle for different values of the parameter α . (b) Asymmetry function of the PDF of the normalized work done by the Gaussian white force on the cantilever for different values of the parameter α . The thick solid line represents the analytical expression given by eq. (11).

viscous dissipation whereas its coupling with the external forcing plays the role of a non-equilibrium thermal bath at an effective temperature² $k\langle x^2 \rangle / k_B = (1 + \alpha)T \approx \alpha T$. The prefactor τ_c / τ is introduced in such a way that w_τ^* represents the average normalized work done during the largest correlation time of the system. Accordingly, the asymmetry function must be redefined as

$$\rho^*(w^*) = \lim_{\tau/\tau_c \rightarrow \infty} \frac{\tau_c}{\tau} \ln \frac{P(w_\tau^* = w^*)}{P(w_\tau^* = -w^*)}. \quad (10)$$

Figure 6(a) shows the asymmetry function ρ^* for the normalized work w_τ^* on the colloidal particle at large values of α for which eq. (6) is violated. The timescale τ_c in the computation of (9) and (10) is taken as the correlation time ($\tau_0 = 25$ ms) of the Ornstein-Uhlenbeck forcing of eq. (2). For comparison we also show the corresponding curves at $\alpha = 0.20, 0.51$ as blue circles and red squares respectively, for which eq. (6) holds. The convergence to a master curve is verified, which means that for a sufficiently strong forcing the thermal bath acts only as a passive

²The parameter α is an unambiguous choice to define the effective temperature out of equilibrium both for the harmonic oscillator and the trapped Brownian particle since $\langle x^2 \rangle$ is finite.

reservoir for the energy dissipation without providing any important contribution to the energy injection into the system. Evidently, the normalized asymmetry function for the values α that verify the FT lie far from the master curve. We point out that the transition to the limit $\alpha \gg 1$ is rather continuous since intermediate regimes occur, as observed for $\alpha = 1.84$. In this case neither the FT is satisfied as shown previously in fig. 3 nor the master curve is attained since the strength of thermal noise is still comparable to that of the external noise.

The results for the normalized asymmetry function of the work done on the cantilever by the external force are shown in fig. 6(b). The curve corresponding to the verification of the FT for $\alpha = 0.19$ is also plotted for comparison. The convergence to a master curve is also checked as the value of α increases. Indeed, when comparing our normalized experimental curves with the analytic expression carried out by [13] for the asymmetry function of the work distribution on a Brownian particle driven entirely by a Gaussian white noise

$$\rho^*(w^*) = \begin{cases} 4w^* & w^* < 1/3 \\ \frac{7}{4}w^* + \frac{3}{2} - \frac{1}{4w^*} & w^* \geq 1/3 \end{cases}, \quad (11)$$

we check that the assumption of the convergence of the energy injection process into the cantilever to that of a Langevin dynamics for a harmonic oscillator entirely dominated by the external noise is valid. Finite α corrections can be detected for large values of w_τ^* indicating that the thermal bath still influences the energy injection into the cantilever. These corrections seem to vanish as the system is driven farther from equilibrium, as observed in fig. 6 for $\alpha = 22.10$.

Finally, we point out that the profile of the master curve strongly depends on the kind of stochastic force: a Gaussian Ornstein-Uhlenbeck process in the first example and a Gaussian white noise in the second one. Non-Gaussian extensions of the external random force are expected to lead to striking modification of the fluctuation relations in the limit $\alpha \gg 1$, as recently investigated for an asymmetric Poissonian shot noise [12].

Conclusions. – We have studied the FT for the work fluctuations in two experimental systems in contact with a thermal bath and driven out of equilibrium by a stochastic force. The main result of our study is that the validity of FT is controlled by the parameter α . For small $\alpha \lesssim 1$ we have shown that the validity of the steady-state FT is a very robust result regardless of the details of the intrinsic dynamics of the system (first- and second-order Langevin dynamics) and the statistical properties of the forcing (white and colored Gaussian noise). Indeed these specific features vanish when the integration of w_τ is performed for τ much larger than the largest correlation time of the system.

In contrast for large $\alpha \gtrsim 1$, when the randomness of the system becomes dominated by the external stochastic

forcing, we have shown that FT is violated. For $\alpha \gg 1$ the results at different driving amplitudes can be set on a master curve by defining a suitable effective temperature which is a function of α . We have shown that this master curve is system dependent.

REFERENCES

- [1] KURCHAN J., *J. Stat. Mech.*, (2007) P07005.
- [2] EVANS D. J. and SEARLES D. J., *Phys. Rev. E*, **50** (1994) 1645.
- [3] GALLAVOTTI G. and COHEN E. G. D., *Phys. Rev. Lett.*, **74** (1995) 2694.
- [4] FEITOSA K. and MENON N., *Phys. Rev. Lett.*, **92** (2004) 164301.
- [5] WANG G. M., REID J. C., CARBERRY D. M., WILLIAMS D. R. M., SEVICK E. M. and EVANS D. J., *Phys. Rev. E*, **71** (2005) 046142.
- [6] GARNIER N. and CILIBERTO S., *Phys. Rev. E*, **71** (2005) 060101(R).
- [7] JOUBAUD S., GARNIER N. B. and CILIBERTO S., *J. Stat. Mech.* (2007) P09018.
- [8] JOP P., PETROSYAN A. and CILIBERTO S., *EPL*, **81** (2008) 50005.
- [9] SEIFERT U., *Phys. Rev. Lett.*, **95** (2005) 040602.
- [10] ZAMPONI F., BONETTO F., CUGLIANDOLO L. F. and KURCHAN J., *J. Stat. Mech.* (2005) P09013.
- [11] TOUCHETTE H. and COHEN E. G. D., *Phys. Rev. E*, **76** (2007) 020101(R); CHECHKIN A. V. and KLAGES R., *J. Stat. Mech.* (2009) L03002.
- [12] BAULE A. and COHEN E. G. D., *Phys. Rev. E*, **80** (2009) 011110.
- [13] FARAGO J., *J. Stat. Phys.*, **107** (2002) 781.
- [14] FARAGO J., *Physica A*, **331** (2004) 69.
- [15] SHANG X.-D., TONG P. and XIA K.-Q., *Phys. Rev. E*, **72** (2005) 015301(R).
- [16] FALCON E., AUMAÎTRE S., FALCÓN C., LAROCHE C. and FAUVE S., *Phys. Rev. Lett.*, **100** (2008) 064503.
- [17] CADOT O., BOUDAUD A. and TOUZÉ C., *Eur. Phys. J. B*, **66** (2008) 399.
- [18] FALCÓN C. and FALCON E., *Phys. Rev. E*, **79** (2009) 041110.
- [19] BONALDI M., CONTI L., DE GREGORIO P., RONDONI L., VEDOVATO G., VINANTE A., BIGNOTTO M., CERDONIO M., FALFERI P., LIGUORI N., LONGO S., MEZZENA R., ORTOLAN A., PRODI G. A., SALEMI F., TAFFARELLO L., VITALE S. and ZENDRI J.-P., *Phys. Rev. Lett.*, **103** (2009) 010601.
- [20] JOP P., GOMEZ-SOLANO J. R., PETROSYAN A. and CILIBERTO S., *J. Stat. Mech.* (2009) P04012.
- [21] BLICKLE V., SPECK T., HELDEN L., SEIFERT U. and BECHINGER C., *Phys. Rev. Lett.*, **96** (2006) 070603.
- [22] PAOLINO P. and BELLON L., in preparation (2009).
- [23] SCHONENBERGER C. and ALVARADO S. F., *Rev. Sci. Instrum.*, **60** (1989) 3131.
- [24] BELLON L., CILIBERTO S., BOUBAKER H. and GUYON L., *Opt. Commun.*, **207** (2002) 49.
- [25] PAOLINO P. and BELLON L., *Nanotechnology*, **20** (2009) 405705.
- [26] BELLON L., *J. Appl. Phys.*, **104** (2008) 104906.